Dual roles for the trimeric G protein Go in asymmetric cell division in *Drosophila*

Vladimir L. Katanaev* and Andrew Tomlinson†

Department of Genetics and Development, College of Physicians and Surgeons, Columbia University, 701 West 168th Street, Suite 1120, New York, NY 10032

During asymmetric division, a cell polarizes and differentially distributes components to its opposite ends. The subsequent division differentially segregates the two component pools to the daughters, which thereby inherit different developmental directives. In *Drosophila* sensory organ precursor cells, the localization of Numb protein to the cell's anterior cortex is a key patterning event and is achieved by the combined action of many proteins, including Pins, which itself is localized anteriorly. Here, a role is described for the trimeric G protein Go in the anterior localization of Numb and daughter cell fate specification. Go is shown to interact with Pins. In addition to a role in recruiting Numb to an asymmetric location in the cell's cortex, Go transduces a signal from the Frizzled receptor that directs the position in which the complex forms. Thus, Go likely integrates the signaling that directs the formation of the complex with the signaling that directs where the complex forms.

Frizzled | cell polarization | signal transduction

Fig. 1. Schematic of SOP divisions and resulting sense organs. Double-headed arrows indicate axes of division.

Cells have the ability to polarize; they differentially segregate subcellular components to opposite ends and establish a clear molecular (and often morphological) asymmetry (1). Such polarizations underlie a host of important biological phenomena, including chemotaxis, axon growth cone guidance, and yeast mating (2–4). Because cell polarization underlies so many biological processes, much work is currently directed to understanding its general principles.

Polarizations can be categorized into a number of different types. For example, in chemotaxis, cells are locomotory; they polarize and move in response to the gradient of an extracellular molecule (2). Contrastingly, in planar cell polarity (PCP), cells are constrained within an epithelium, and, in response to an inferred extracellular signal, they polarize within the plane of the epithelium and secrete hairs or bristles in a uniform direction (5). Although a role for an extracellular signal is common to both these types, it is important to note that it only plays a coordinating role. Cells can polarize in the absence of extracellular information; the polarizations just occur in random orientations. Thus, the extracellular information directs the orientation of the polarization, not the mechanism of polarization itself.

Asymmetric cell division (6–8) is another example in which cell polarization plays a critical role. Here, cell fate determinants become partitioned to opposite ends of a cell, and subsequent cell division leads the differential inheritance of fate-directing components by the daughters. In *Drosophila*, two different types of asymmetric divisions have been defined by the initial orientation of polarization. One type is represented by neuroblasts, which delaminate from the embryonic neuroectoderm and divide repeatedly in the apical/basal axis to generate the cells of the CNS. The other type is represented by the sensory organ precursor cells (SOPs), which divide asymmetrically to generate the four cells (external hair and socket cells and internal neuron and sheath cells) of adult sensory structures (Fig. 1). Unlike neuroblasts, SOPs are polarized and divide in the plane of the epithelium. Of the two SOP daughter cells, pIIa also divides within the plane of the epithelium, but pIIb and its derivative,
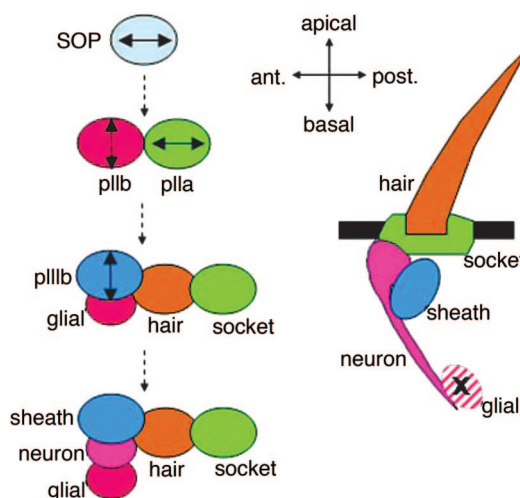
pIIIb, divide apically/basally (9). In addition to the axis of division, the two types of asymmetric cell divisions differ in their progeny size; SOPs generate daughters of equal size, and neuroblasts generate daughters of different sizes.

SOP divisions and PCP share the common feature of polarization in the plane of the epithelium. In PCP, a unique position is defined within an epithelial cell from which a structure such as a hair is secreted. Collectively, the cells of the epithelium coordinate their polarizations such that all cells secrete the hairs in the same direction. When the Frizzled (Fz) receptor is removed from these cells, each is still largely capable of polarizing and secreting a hair from a unique position, but the coordination is lost; the hairs are no longer uniformly arranged (10). Similarly, in *fz* mutants, the SOPs still polarize and divide asymmetrically; it is the correct orientation of the asymmetry that is lost (11). By inference, then, the axis of polarization of SOPs and cells of PCP are regulated by extracellular information transduced through the Fz receptor.

Trimeric G proteins are composed of a guanine nucleotide-binding α-subunit and a βγ heterodimer. In the resting state, the α-subunit is GDP-bound and associated with a seven-transmembrane helix receptor. Activation of the receptor catalyzes exchange of GDP on the α-subunit, and subsequent dissociation of the
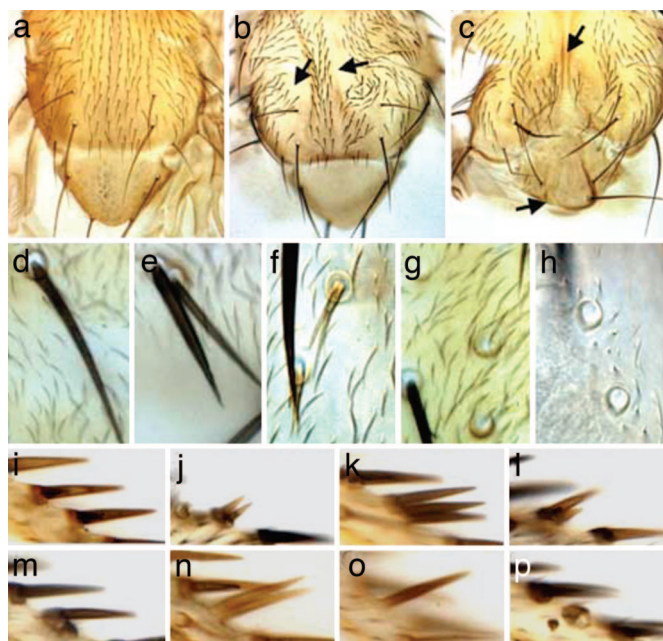
Fig. 2. Loss of function and overexpression of Go cause orientation and asymmetric division defects. (*a*) Adult WT thorax. Macrochaetae and microchaetae show stereotypical posterior orientation. (*b*) Thorax with *Go* mutant clones show bald regions (arrows), and surviving bristles are small and misoriented. (*c*) Thorax of a *pnr-Gal4, UAS-Go^{GTP}* fly. Bristle orientation defects occur, as well as bald regions (arrows). *pnr-Gal4* drives in eight thoracic macrochaetae; on average, 15% of these macrochaetae were lost per thorax, and all thoraces lost at least one macrochaeta. (*d*) A WT thoracic bristle (microchaeta) at high resolution, showing external socket and a hair. (*e–h*) Bristle structures resulting from overexpression of *Go^{GTP}* (*e* and *g*) or loss of *Go* (*f* and *h*) (late clones). Defective bristles may contain two sockets/two hairs (*e*), one socket/two hairs (*f*), or one socket/no hair (*g* and *h*). Three percent of *pnr-Gal4, UAS-Go^{GTP}* bristles and 8% of *Go* bristles had hair/socket duplications. Socket-only phenotype occurred at rates of 24% and 5%, respectively. (*i–p*) Wing margin stout bristles: WT (*i*), *Go* (*j* and *l*), or *UAS-Go^{WT}* or *UAS-Go^{GTP}* (*k* and *m–p*). Defective bristles may contain two sockets/two hairs (*j*), one socket/three hairs (*k*), one socket/two hairs (*l*), two sockets/one hair (*m*), no socket/two hairs (*n*), no socket/one hair (*o*), or one or two sockets/no hair (*p*). *MS1096-Gal4* driving a single copy of *UAS-Go^{WT}* or *UAS-Go^{GTP}* affected 1.5% and 3% of margin bristles, respectively. All wings had at least one defective margin bristle. Wing margin defects of *Go* clones (16) prevented an assessment of frequency of defects.

complex releases free Gα-GTP and βγ, which can then engage downstream targets. With time, Gα hydrolyzes GTP back to GDP, and the Gα-GDP–βγ trimeric complex reforms (12). The actions of trimeric G proteins have been extensively implicated in the diverse examples of polarization (2, 13–15). Fz signaling in *Drosophila* (in both the PCP and Wnt pathways) has recently been shown to depend on the trimeric G protein Gαo (Go) (16), and because Fz receptor function controls the orientation of asymmetric SOP divisions, we investigated any function for Go in the processes of asymmetric cell division. Here, we describe roles for Go not only in the orientation mechanism (transducing the Fz signal) but also in the mechanism of polarization itself. This latter mechanism had previously been thought to depend on another Gα-subunit, Gi (17, 18), but our data suggest that Go plays the more pervasive role. Because Go appears to act in the two distinct aspects of SOP asymmetry (the orientation and the polarization itself), it is a potential integrator of the two pathways, working in the establishment of the asymmetry and sensing and responding to the orientation signal.

Results

Go Mutant SOPs Show both Orientation and Asymmetry Defects. SOP
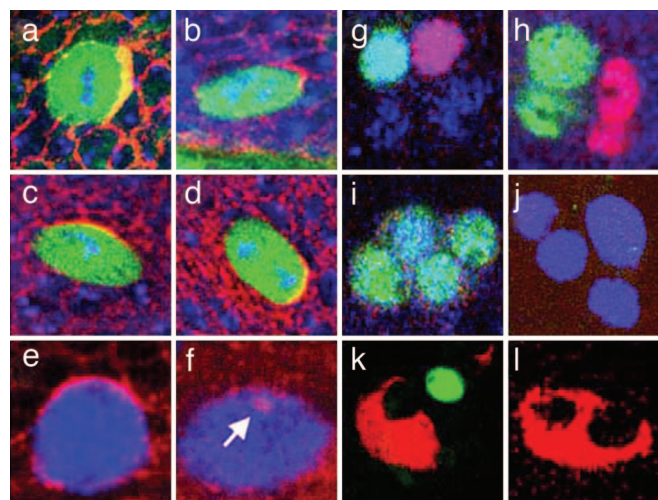derivatives were examined in clones that were mutant for *Go* or

Fig. 3. Loss and overexpression of Go causes aberrant SOP Numb crescents and aberrant cell specification. (*a–d*) Dorsocentral SOPs in metaphase (*a* and *c*) and early telophase (*b* and *d*) stained for DNA (blue), Sens (green), and Numb (red) in WT (*a* and *b*) and *UAS-Go^{WT}* (*c* and *d*) cells. Anterior is to the right. *UAS-Go^{WT}* SOPs show Numb crescents in variable positions. (*e* and *f*) Overexpression of *Go^{GTP}* in mitotic SOPs (α-Sens, blue) leads to severe defects in Numb localization (red), such as near-ubiquitous plasma membrane staining (*e*) or loss from the plasma membrane (*f*), sometimes with intracellular vesicular staining (arrow). (*g–j*) Four-cell bristle clusters resulting from SOP divisions stained with α-Sens (blue) at ≈25 h APF. (*g*) WT contains two internal cells, neuron (α-Elav, green) and a sheath cell (α-Pros, red), and two external cells. (*h*) In *UAS-Go^{GTP}*, internal cells often duplicate at the expense of external cells, forming two neuronal (green) and two sheath (red) cells. In *sca-Gal4, UAS-Go^{GTP}* this transformation occurred in ≈10% of bristles. (*i*) Rarely (≈1%), four neurons form. (*j*) *UAS-Go^{GTP}* can induce duplication of external cells, resulting in clustered Sens-positive cells (blue) not expressing internal cell markers. α-Sens staining begins to decay at this stage, preventing an assessment of the frequency of this occurrence. (*k* and *l*) Shown is ≈35-h APF staining with α-Su(H) (socket cell, red) and α-Elav (neuron, green). WT clusters have a single socket and a single neuron cell (*k*), whereas ≈4% of *UAS-Go^{GTP}* clusters lose neurons and duplicate the socket cells (*l*).

were overexpressing different forms [*Go^{WT}* or *Go^{GTP}* (the activated form of Go)] of the protein. In addition to polarity effects (orientation of the bristles; Fig. 2 *b* and *c*), defects consistent with asymmetric division aberrations were observed. These defects included absence of the external cells (arrows in Fig. 2 *b* and *c*), duplicated sockets and/or hairs (Fig. 2 *e, f,* and *j–n*), and bristles devoid of sockets or hairs (Fig. 2 *g, h,* and *n–p*). The loss-of-function clones and the overexpressions varied in their potency, but all induced the range of phenotypes described above. Loss or duplication of external bristle cells is observed when Numb activity is similarly modulated (19, 20).

Numb is a phosphotyrosine-binding protein that regulates Notch activity (20–22), and the localization of Numb to a crescent of the SOP anterior cortex ensures its specific inheritance by pIIb (19). In WT mitotic SOPs, the crescent of Numb was found robustly anterior (Fig. 3 *a* and *b*), but when Go levels were modulated, it was found at many positions in the cell cortex (Fig. 3 *c* and *d*). These results are consistent with a role for Go in transducing the Fz orientation signal. In addition to mispositioning of the Numb crescent, modulation of Go often resulted in more severe defects. Specifically, mitotic SOPs showed multiple crescents, near-ubiquitous cortical Numb staining (Fig. 3*e*), or a strong reduction of cortical staining with occasional concomitant Numb-positive vesicle-like structures (Fig. 3*f*, arrow).

The crescent defects described would be expected to lead to pIIa inheriting too much Numb or pIIb inheriting too little Numb. Cell type markers were used to ascertain cell fates in developing thoracic four-cell bristle groups identified by their Senseless expression at
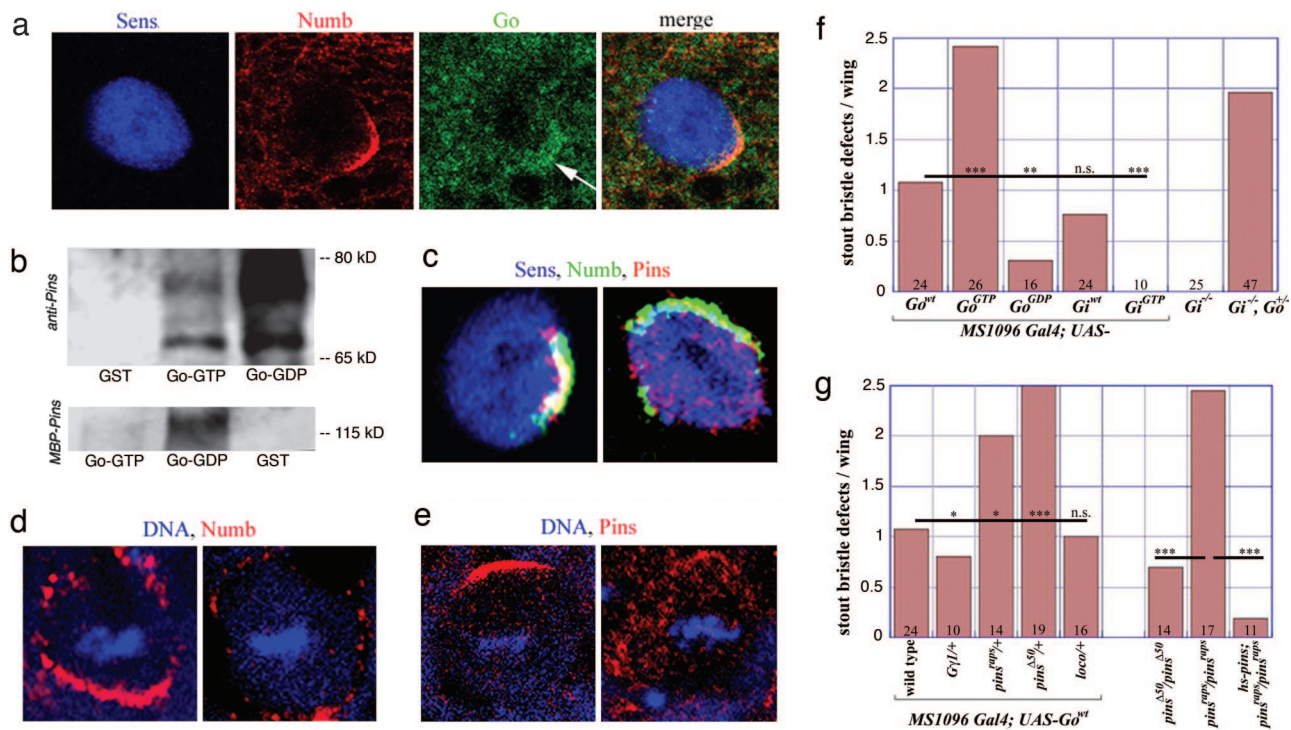
Fig. 4. Localization and biochemical/genetic interactions of Go in SOPs. (*a*) In a mitotic SOP (α-Sens, blue), Go protein (green) can form an anterior cortical crescent (arrow) overlapping with the Numb (red). (*b*) (*Upper*) Go-GTP resin and Go-GDP resin, but not GST resin, precipitate full-length Pins (≈70 kDa) from *Drosophila* extracts. Go-GDP (more effectively than Go-GTP) binds a slower migrating, phosphatase-sensitive form of Pins (≈75 kDa). (*Lower*) Go-GDP binds purified MBP-Pins; Go-GTP binds much less. Equal amounts of GST and GST-Go protein were loaded in each lane. (*c*) In WT (*Left*), Pins (red) localizes in an anterior crescent in mitotic SOPs (α-Sens, blue), colocalizing with Numb (green; yellow in merge). Overexpression of Go (*UAS-GoWT*, *Right*) decreases plasma membrane localization of Pins. Numb crescent formation is disturbed less. (*d* and *e*) WT (*Left*) and *sca-Gal4; UAS-GoGTP* (*Right*) neuroblasts stained for Numb (*d*, red) or Pins (*e*, red) and DNA (blue); apical is up. (*f*) Quantification of stout bristle asymmetric division defects upon overexpression of different forms of Go and Gi and in *Gi* homozygotes. GoGTP, but not GiGTP, induces asymmetric division defects. Removal of Gi produces phenotypes only in *Go* heterozygotes. Mean values are shown as bars; numbers indicate the number of wings analyzed for each genotype. Statistical significance was assessed by unpaired *t* test. ∗∗∗, $P < 0.005$; ∗∗, $P < 0.01$; ∗, $P < 0.05$; n.s., $P > 0.1$. (*g*) Overexpressed Go-induced division defects are attenuated by removal of one copy of Gγ1, strongly enhanced by *pins*, and unaffected by *loco*. Removal of *pins* produces frequent bristle defects, rescued by a *hsp70-pins* transgene.

≈25 h after puparium formation (APF). In WT, a single Prospero-positive cell (sheath) and a single Elav-positive cell (neuron) were identified (Fig. 3g). But, when Go levels were modulated, clusters containing only internal cells (two sheath cells and two neurons) were often found (Fig. 3h). More rarely, clusters containing four neurons were observed (Fig. 3i), suggesting defects in the subsequent pIIb asymmetric divisions. These duplications of the internal cells at the expense of the external cells are consistent with the bald patches seen in the adult tissues (Fig. 2 b and c) and result from pIIa-to-pIIb transformations.

If SOP divisions resulted in neither daughter inheriting sufficient levels of Numb, then the opposite pIIb-to-pIIa cell fate transformation should occur, resulting in the duplication of external cells. Four-cell clusters were identified that stained with α-Senseless but not with any internal cell markers (Fig. 3j). These clusters represent duplicated external cells (with complete loss of internal cells) that would result in the duplications of the adult external bristle cells shown in Fig. 2. Further evidence was provided by costaining at ≈35 h APF with α-Su(H), which selectively labels socket cells and α-Elav to stain neurons (see Fig. 3k for a WT staining). Upon expression of GoGTP, we observed clusters lacking α-Elav staining but showing two Su(H)-positive cells, indicating duplication of external cells at the expense of the internal cells (Fig. 3l).

Asymmetric Go Localization. The observation that modulations of Go activity could affect Numb localization raised the question of whether Go itself was asymmetrically distributed. Mitotic dorso-central macrochaetae SOPs were stained with α-Go, and a general cytoplasmic distribution that was stronger in the cortical regions was observed. In ≈50% of SOPs examined, Go protein was enriched in the anterior cortex overlapping with the Numb crescents (Fig. 4a).

Go and Gi Genetically Interact. In addition to Go, another Gα-subunit, Gαi (Gi), has previously been implicated in asymmetric divisions (17, 18). Gi and Go differ significantly in their phenotypic effects. *Gi* mutants show no bristle orientation phenotypes, and although they show metaphase defects in localization of cell fate determinants (17, 18), normal distributions are restored by telophase, and no adult defects occur (see Fig. 4f). As described above, overexpression of GoWT or GoGTP produced asymmetric cell division phenotypes, but only overexpression of the WT Gi (not the GTP form) induced phenotypes (Fig. 4f). Because the "activated" form of Gi was impotent, the effects of the WT form likely resulted from the sequestration of βγ moieties required by other α-subunits such as Go. Thus, Go and Gi do not appear to play equivalent roles. However, removal of one gene copy of *Go* in *Gi* homozygotes resulted in adult bristle defects (Fig. 4f). Whether Go and Gi are partially redundant in one or other function remains unclear, but the stronger effects of Go suggest that it plays the more pervasive role in the SOP asymmetric mechanism.

Go Binds to Pins and Interacts with It Genetically. Pins is a protein of the anterior complex that recruits Numb (23) and contains GoLoco motifs, domains that are known to interact with G proteins of the Gαi/o class (24). Pins binds both Gi and Go in reticulocyte lysates (25) and in yeast two-hybrid assays (26, 27). The isolated Pins

GoLoco binds GDP-loaded Gi but not GTP-loaded Gi (17). We tested whether Go could coprecipitate Pins from *Drosophila* extracts. Both GTP-loaded and GDP-loaded Go precipitated Pins at the expected size ($\approx$70 kDa; Fig. 4b *Upper*), and a second, phosphatase-sensitive, slower migrating form of Pins was precipitated preferentially by Go-GDP (Fig. 4b *Upper*). Although the physiological significance of this phosphorylated form of Pins and its binding to Go-GDP remains unclear, the differential binding activities of the GDP and GTP forms of Go suggest a specific and regulated interaction with Pins.

With a single exception (28), all previously described GoLoco domain-containing proteins are known to interact exclusively with GDP-loaded Gα-subunits (24), and yet here, GTP-loaded Go effectively precipitated Pins. We therefore examined the interaction of bacterially expressed and purified Pins and Go. Here, Go-GDP bound Pins at least one order of magnitude more effectively than Go-GTP (Fig. 4b *Lower*). Thus, Go-GTP binds Pins from fly extracts much more effectively than does a bacterially generated Pins. Whether this effect relates to folding differences in the bacterially expressed proteins or the presence of some stimulator of Go-GTP/Pins interaction in the fly extracts remains unclear.

Given the coprecipitation of Go and Pins, we looked for genetic interaction between the two. When Go was overexpressed in a *pins* heterozygous background, a significant enhancement of the asymmetric division effects was observed (Fig. 4g; two different alleles of *pins* behaved similarly). In contrast, no modification of the Go overexpression phenotypes was observed when a single copy of another GoLoco-encoding gene, *loco* (29), was removed. Furthermore, overexpression of Go disturbed localization of Pins more readily than that of Numb (Fig. 4c).

If Go directs the formation of the Numb crescent by appropriately localizing Pins, then *pins* mutants should phenocopy the effects of Go. Animals homozygous for the hypomorphic $\Delta50$ *pins* allele (25) show only rare defects in asymmetric divisions in the wing margin (Fig. 4g), but over a null allele [*raps193* (26)], transheterozygotic animals showed extensive asymmetric division phenotypes in all tissues analyzed; Fig. 4g quantifies the effects in the wing margin. These phenotypes were rescued by the presence of an *hsp70-pins* transgene (Fig. 4g). Homozygous clonal tissues of the *raps193* allele showed the phenotypes observed in the transheterozygotes (not shown).

There are four pieces of evidence linking Pins and Go: (*i*) they interact genetically, showing synergistic effects, (*ii*) they phenocopy each other's mutant effects, (*iii*) Pins is delocalized when Go is overexpressed, and (*iv*) Pins and Go coprecipitate. Collectively, these observations argue that Go and Pins are critical partners in the establishment of the Numb crescent.

Go Function also Is Required for Neuroblast Asymmetric Cell Divisions.

Because Go functioned in the establishment of SOP asymmetry (in addition to its orientation), we wondered whether it played a similar role in the neuroblast divisions.

Perdurance of maternal gene function masks any role for Go in early embryonic stages, including the neuroblast divisions, and *Go* germ-line mutant clones cannot be generated (16). We therefore examined neuroblasts in which Go^{GTP} was overexpressed. In WT neuroblasts, Numb localizes to the basal cortex, whereas Pins localizes apically (25, 26, 19) (Fig. 4 *d Left* and *e Left*). However, expression of Go^{GTP} caused both proteins to become diffuse (Fig. 4 *d Right* and *e Right*). Without the loss-of-function analysis, we cannot conclude that Go is critically required for the neuroblast divisions, but the effects of overexpression of Go^{GTP} are consistent with this inference.

The Overexpression Effects of Go Require Fz.

Because Fz appears to act as the exchange factor for Go in the Wnt and PCP pathways (16), we examined the effects of Go^{WT} and Go^{GTP} on wing margin bristles when Fz levels were modulated. The effects of overexpression of Go^{WT} fell to zero in $fz^{-/-}$ wings, but the Go^{GTP} overexpression phenotypes were not reduced; rather, they were enhanced (Fig. 5 *a–d* and *g*). Why the aberrations increased is not clear, but this result shows that Go^{GTP} is a potent disturber of asymmetric division in the absence of Fz, whereas WT Go requires it. This finding suggests that Go requires Fz to convert it into the "active" GTP-bound state and predicts that overexpression of Fz should enhance the potency of Go. Indeed, co-overexpression of Fz and Go^{WT} enhanced the asymmetric division defects (Fig. 5 *e–g*). Overexpression of Fz alone produced orientation defects but no asymmetric division aberrations (Fig. 5h).

Both Fz and Dfz2 (*Drosophila* Fz 2) Appear as Exchange Factors for Go in the SOPs.

In *Drosophila*, Wnt-1 (Wingless, Wg) is transduced by the Go-dependent receptors Fz and Dfz2 (16). We therefore tested whether co-overexpression of Dfz2 could also enhance the effects of overexpression of Go. Overexpression of Dfz2 alone characteristically induced ectopic margin bristles [activation of the Wg pathway (30)] that showed no asymmetric division defects (Fig. 5i). But when Dfz2 and Go^{WT} were co-overexpressed, they mutually enhanced their respective phenotypes (Fig. 5 *j* and *g*), suggesting that Go enhanced the ability of Dfz2 to ectopically activate Wg signaling, and Dfz2 potentiated the ability of Go to disturb the asymmetric divisions. Dfz2 is usually down-regulated in the SOP region of the wing margin (30) and likely does not normally influence Go activity there, but its forced expression shows an ability to potentiate the effects of Go (by inference catalyzing it into the GTP-activated form). To our knowledge, these results provide the first example of the ability of Dfz2 to activate signaling in a pathway other than "canonical" Wnt cascade.

Gβ13F and Gγ1 Likely Represent the β- and γ-Subunits of the Go Trimeric Complex.

Receptor-catalyzed exchange of GDP for GTP occurs on Gα-subunits complexed with $\beta\gamma$. Thus, $\beta\gamma$-subunits should be required for the effects of Go^{WT} overexpression. Indeed, Go^{WT} overexpression effects were attenuated when one gene copy of *Gγ1* was removed (Fig. 4g), arguing that these effects were not due to sequestration of $\beta\gamma$ moieties from another α-subunit such as Gi. Ablation of Gβ13F or Gγ1 genes was reported to affect neuroblast divisions (17, 18, 31). We also found that loss or overexpression of Gγ1 and Gβ13F (but not Gβ5) resulted in adult bristle defects similar to those of loss or overexpression of Go (data not shown). Taken together, these observations suggest that Gβ13F and Gγ1 represent the β- and γ-subunits of the Go trimeric complex.

Discussion

Various roles for trimeric G proteins have previously been reported for asymmetric cell divisions (15); for example, *Caenorhabditis elegans* Gα-subunits GOA-1 and GPA-16 redundantly regulate posterior displacement of the mitotic spindle required for the asymmetric division of the zygote, and β- and γ-subunits are involved in orientating the mitotic spindle (32). In *Drosophila*, evidence for trimeric G protein function in both the formation of the asymmetric spindle and the correct localization of various cell fate determinants came from manipulation of $\beta\gamma$-subunits in the neuroblasts (17, 18, 31, 33). Additionally, Gi was known to be involved in asymmetric divisions and to interact with Pins (17, 18); cell fate determinant localizations were aberrant during metaphase but were restored by telophase (18).

In this report, we document strong and pervasive roles for Go in *Drosophila* asymmetric divisions. We make five major points:

1. In SOP asymmetric divisions, there are two patterning mechanisms: the establishment of the asymmetric complexes and the orientation of the asymmetry. Go appears to act in both functions and is therefore a likely molecular integrator of the two.
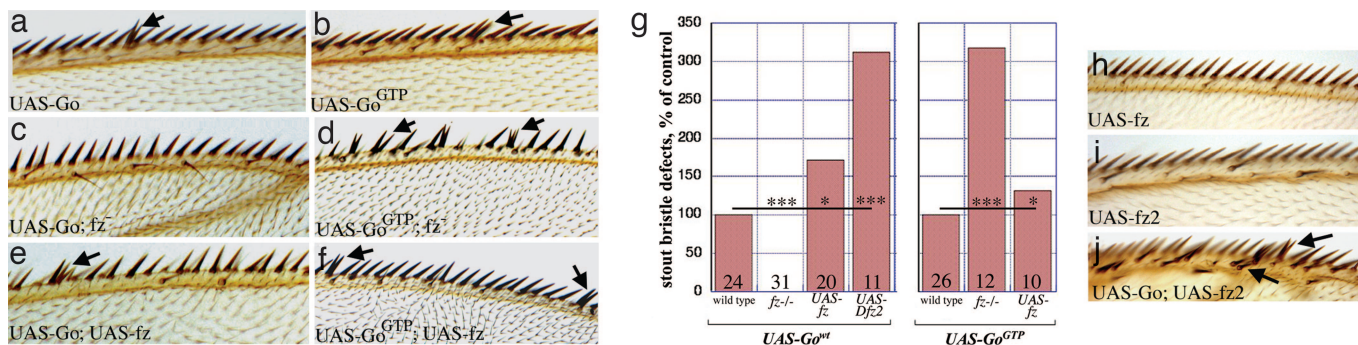
Fig. 5. Genetic interactions of Go with Fz receptors. (*a–d*) Removal of *fz* rescues asymmetric cell division defects of *UAS-Go^{WT}* (*a* and *c*) but not *UAS-Go^{GTP}* (*b* and *d*). (*e*, *f*, and *h–j*) Coexpression of *UAS-fz* enhances both phenotypes (*e* and *f*), whereas *UAS-fz* alone does not produce any asymmetric division defects (*h*). Expression of Dfz2 produces ectopic margin bristles (*i*), whereas co-overexpression of Go and Dfz2 results in mutual enhancement of both division and ectopic bristle phenotypes (*j*, arrows). (*g*) Division defects are quantified, normalizing *UAS-Go^{WT}* and *UAS-Go^{GTP}* as 100%. Data are presented as in Fig. 4.

2. Go appears to function in both the neuroblast-type and SOP divisions and is therefore likely used in all asymmetric divisions in *Drosophila*.

3. Go binds to and genetically interacts with Pins. One function of Go, then, is likely mediated by a direct interaction with Pins.

4. Hitherto, Gi was considered the major Gα-subunit functioning in asymmetric cell divisions. Go shows significantly stronger phenotypes, suggesting a greater role, but genetic interaction between the two suggests a degree of functional redundancy.

5. Both Fz and Dfz2 appear able to act as exchange factors for Go in the SOP divisions. The role for Fz is supported by many different results, but whether Dfz2 normally functions here remains unclear.

Go appears to play parallel bifunctional roles in the establishment of asymmetries in both SOPs and PCP (Fig. 6), as evidenced by the following. First, polarized structures form in both; in PCP, it is the focal organizer of hair outgrowth, and in SOPs, it is the Numb crescent (Fig. 6 *Left*). Second, in both processes, Fz signaling organizes the polarized distribution of "core group" PCP proteins (5). For example, Fz itself becomes localized to the distal and posterior ends of PCP cells and SOPs, respectively (shown in green in Fig. 6) (34, 35), whereas Van Gogh/Strabismus is found proximal and anterior in PCP cells and SOPs, respectively (35, 36). Third, in both processes, these Fz-dependent localizations do not critically contribute to the final polarized structures, because loss of Fz (or other core group proteins) only leads to randomization in the positioning of the (usually) single-hair focus or Numb complex (Fig. 6 *Center*) (10, 11, 37). Thus, there appear to be two semiindependent mechanisms: (*i*) the polarization of the core group PCP proteins, which instructs (*ii*) the position of the self-assembling complexes.

Go appears to work in both these mechanisms. Mildly Go-compromised cells lose correct orientation of hairs (16) or Numb complexes, consistent with an orientation function. Cells with strongly disturbed Go function lose the ability to polarize (Fig. 6 *Right*); in the SOP, Numb becomes diffuse or forms a number of small foci (Fig. 6*a*); and in PCP, many hair initiation sites are produced (16) (Fig. 6*b*). Phenotypes of *fz* or other core group mutants occasionally result in two hairs per cell (37), but *Go* mutants frequently induce cells with five or six hairs (16).

The question now arises as to whether Go functions in the same way in both processes. In terms of the Fz-mediated orientation step, it is likely that Go performs the same role; in both, Fz is directed to one end of the cell (distal or posterior) (34, 35), and Go itself becomes preferentially distributed to the other end (proximal or anterior) (16). This local enrichment of Go possibly serves as the point of integration with the internal asymmetry formation step. In the SOP case, anterior Go may recruit Pins and seed the formation of the anterior Numb crescent. In the PCP case, Go localizes opposite to the site of hair growth, suggesting that the highest depletion of Go specifies the site of hair growth. In the absence of the Fz orienting information, it may be a stochastic increase of Go localization (or
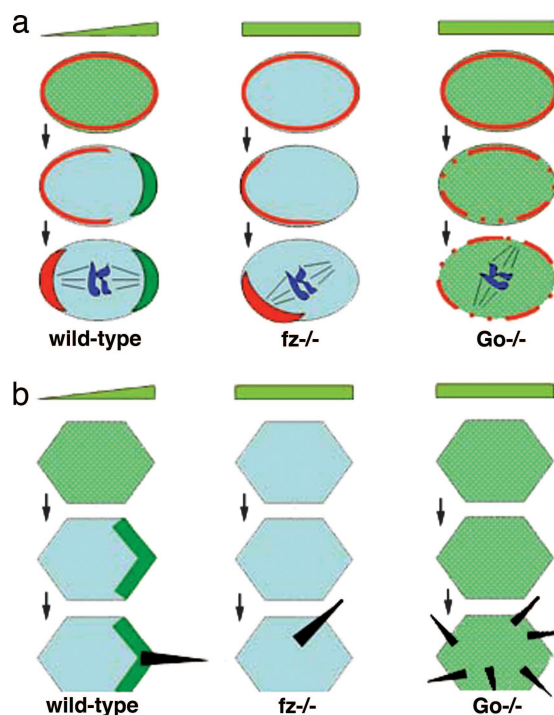

Fig. 6. Schematic comparison of the *fz* and *Go* phenotypes in SOP divisions (*a*) and the PCP mechanism (*b*). (*Left*) In the WT SOP (*a*) and wing epithelial cell (*b*), a gradient of an extracellular signal (schematized by the light-green triangle) is likely decoded by Fz (originally equally distributed around the cell surface, schematized by the green shading). This decoding results in a posterior (SOP) or distal (PCP) enrichment of Fz (schematized by the dark-green accumulations), followed by anterior localization of the Numb crescent (red in *a*) and distal localization of the hair growth site (black in *b*). (*Center*) In the absence of Fz, cell polarization still occurs because of the intrinsic cell polarization machinery, but at random locations; this phenomenon is illustrated by the improper positioning of the Numb crescent (*a*) or hair growth site (*b*). (*Right*) In *Go* mutants, Fz signaling fails, resulting in failure of Fz to redistribute (illustrated by the persistent green shading). Also, the intrinsic cell polarization machinery is faulty, leading to diffuse or multifocal Numb staining (red in *a*) or formation of multiple hair growth sites (black in *b*).

Katanaev and Tomlinson

activity) that establishes the initial asymmetric bias. Alternatively, the asymmetric distribution of Go may only be a manifestation of the Fz-mediated orientation, being essentially irrelevant to the subsequent step. In this case, the activity of Go (rather than its site of accumulation) would be required for the formation of the Numb crescent or the hair initiation point.

Materials and Methods

Genetics. Alleles used were as follows: *Go[007]* (38); *Gi[P20]*, *Gi[P8]*, and *Gi[P29]* (18); *Gγ1[k08017]* (Bloomington Stock Center, Indiana University) and *Gγ1[N159]* (31); *Gβ13F[Δ1-96A]* (17); *pins[Δ50]* (25) and *pins[raps193]* (26); *loco[D13]* and *loco[M1]* (29); and *fz[H51]* and *fz[KD4A]* (39). Mitotic clones were induced as described in ref. 16 at 24–48 h or 48–72 h after egg laying; *Vg-Gal4, UAS-flp* (40) was used to create *Go[007]* clones in the wing with some mutant margin bristles surviving to adulthood. *UAS-β13F* and *UAS-β5* were made by PCR from genomic DNA, followed by subcloning into a transformation vector (41). Other transgenes used were as follows: *UAS-Go^WT, -Go^GTP*, and *-Go^GDP* (16); *UAS-Gi^WT/-Gi^GTP* (17); *UAS-Gγ1* (31); *UAS-Fz* (41) and *UAS-Dfz2* (42); and *hsp70-pins* (26). Thorax and abdomen expression was driven by *pnr-Gal4* or *sca-Gal4* (43). *sca-Gal4* was used for neuroblasts, and *MS1096-Gal4* (44) was used for wings.

Histology. Thoracic macrochaetae and microchaetae SOPs were analyzed at 0 and 16 h APF, respectively. Bristle clusters were stained at 20–30 h APF. Mitotic SOPs were identified by diffuse α-Sens staining and by condensed DNA stained with 0.1 μM TOTO-3 (Molecular Probes). We used the following antibodies: α-Sens (45), α-Numb (19), α-Pins (ref. 26 and from J. Knoblich, Institute of Molecular Pathology, Vienna), α-Pros [Developmental Studies Hybridoma Bank (DSHB), Iowa City, IA], α-Elav (DSHB), α-Go (16), and α-Su(H) (46). Asymmetric division defects in adult wing margins were quantified as the number of stout bristles with defects. Twenty wings were analyzed for each genotype. Stage-10 embryos were immunostained as described in ref. 47.

Biochemistry. Go was subcloned into a pGEX plasmid (Amersham Pharmacia), expressed in *Escherichia coli*, and purified as a GST-fusion protein. GST alone was purified alongside. Preloading with GTPγS or GDPβS (Sigma) was performed as in ref. 48. Biological activity of GST-Go was confirmed by using radioactive GTP (Amersham Pharmacia Biosciences), $\beta\gamma$ (Calbiochem), and pertussis toxin (Sigma). For the adult fly protein extracts, 100–200 flies were homogenized in 5 ml of hypotonic buffer (13.5 mM KCl/1 mM NaCl/0.1 mM DTT/0.2 mM MgCl$_2$/1 mM Hepes/0.2 mM EGTA, pH 7.0) supplemented with complete EDTA-free protease inhibitor mixture (Roche Applied Science, Indianapolis) and centrifuged at $13,000 \times g$ for 20 min at 4°C. Three hundred microliters of fly extracts were incubated overnight at 4°C in PBS/1 mM DTT plus 0.1 mg/ml GST-Go (or the equimolar amount of GST) and 20 μl of glutathione Sepharose 4B (Amersham Pharmacia Biosciences). After three PBS rinses, Sepharose-associated proteins were run on SDS/PAGE. Western blotting was performed with α-Pins. Phosphatase treatment was performed with shrimp alkaline phosphatase (Roche Applied Science). Pins fused to maltose-binding protein (MBP) was expressed in *E. coli* from a pMAL-c2-Pins plasmid (25) and purified on amylase resin (NEB, Beverly, MA). Equimolar amounts of GST-Go (or GST) and MBP-Pins were incubated as above, and proteins associated with glutathione Sepharose were resolved on SDS/PAGE, followed by Coomassie staining. MBP-Pins was identified by its molecular weight and additionally confirmed by Western blotting by using α-Pins or α-MBP (NEB).

CELL BIOLOGY

1. Horvitz, H. R. & Herskowitz, I. (1992) *Cell* **68,** 237–255.
2. Van Haastert, P. J. & Devreotes, P. N. (2004) *Nat. Rev. Mol. Cell Biol.* **5,** 626–634.
3. Huber, A. B., Kolodkin, A. L., Ginty, D. D. & Cloutier, J. F. (2003) *Annu. Rev. Neurosci.* **26,** 509–563.
4. Chant, J. (1999) *Annu. Rev. Cell Dev. Biol.* **15,** 365–391.
5. Adler, P. N. (2002) *Dev. Cell* **2,** 525–535.
6. Betschinger, J. & Knoblich, J. A. (2004) *Curr. Biol.* **14,** R674–R685.
7. Bardin, A. J., Le Borgne, R. & Schweisguth, F. (2004) *Curr. Opin. Neurobiol.* **14,** 6–14.
8. Roegiers, F. & Jan, Y. N. (2004) *Curr. Opin. Cell Biol.* **16,** 195–205.
9. Roegiers, F., Younger-Shepherd, S., Jan, L. Y. & Jan, Y. N. (2001) *Nat. Cell Biol.* **3,** 58–67.
10. Vinson, C. R. & Adler, P. N. (1987) *Nature* **329,** 549–551.
11. Gho, M. & Schweisguth, F. (1998) *Nature* **393,** 178–181.
12. Hepler, J. R. & Gilman, A. G. (1992) *Trends Biochem. Sci.* **17,** 383–387.
13. Dohlman, H. G. (2002) *Annu. Rev. Physiol.* **64,** 129–152.
14. Katanaev, V. L. (2001) *Biochemistry (Moscow)* **66,** 351–368.
15. Hampoelz, B. & Knoblich, J. A. (2004) *Cell* **119,** 453–456.
16. Katanaev, V. L., Ponzielli, R., Semeriva, M. & Tomlinson, A. (2005) *Cell* **120,** 111–122.
17. Schaefer, M., Petronczki, M., Dorner, D., Forte, M. & Knoblich, J. A. (2001) *Cell* **107,** 183–194.
18. Yu, F., Cai, Y., Kaushik, R., Yang, X. & Chia, W. (2003) *J. Cell Biol.* **162,** 623–633.
19. Rhyu, M. S., Jan, L. Y. & Jan, Y. N. (1994) *Cell* **76,** 477–491.
20. Guo, M., Jan, L. Y. & Jan, Y. N. (1996) *Neuron* **17,** 27–41.
21. Spana, E. P. & Doe, C. Q. (1996) *Neuron* **17,** 21–26.
22. Cayouette, M. & Raff, M. (2002) *Nat. Neurosci.* **5,** 1265–1269.
23. Bellaiche, Y., Radovic, A., Woods, D. F., Hough, C. D., Parmentier, M. L., O'Kane, C. J., Bryant, P. J. & Schweisguth, F. (2001) *Cell* **106,** 355–366.
24. Willard, F. S., Kimple, R. J. & Siderovski, D. P. (2004) *Annu. Rev. Biochem.* **73,** 925–951.
25. Schaefer, M., Shevchenko, A. & Knoblich, J. A. (2000) *Curr. Biol.* **10,** 353–362.
26. Parmentier, M. L., Woods, D., Greig, S., Phan, P. G., Radovic, A., Bryant, P. & O'Kane, C. J. (2000) *J. Neurosci.* **20,** 1–5.
27. Giot, L., Bader, J. S., Brouwer, C., Chaudhuri, A., Kuang, B., Li, Y., Hao, Y. L., Ooi, C. E., Godwin, B., Vitols, E., *et al.* (2003) *Science* **302,** 1727–1736.
28. Meng, J., Glick, J. L., Polakis, P. & Casey, P. J. (1999) *J. Biol. Chem.* **274,** 36663–36669.
29. Granderath, S., Stollewerk, A., Greig, S., Goodman, C. S., O'Kane, C. J. & Klambt, C. (1999) *Development (Cambridge, U.K.)* **126,** 1781–1791.
30. Cadigan, K. M., Fish, M. P., Rulifson, E. J. & Nusse, R. (1998) *Cell* **93,** 767–777.
31. Izumi, Y., Ohta, N., Itoh-Furuya, A., Fuse, N. & Matsuzaki, F. (2004) *J. Cell Biol.* **164,** 729–738.
32. Gotta, M. & Ahringer, J. (2001) *Nat. Cell Biol.* **3,** 297–300.
33. Fuse, N., Hisata, K., Katzen, A. L. & Matsuzaki, F. (2003) *Curr. Biol.* **13,** 947–954.
34. Strutt, D. I. (2001) *Mol. Cell* **7,** 367–375.
35. Bellaiche, Y., Beaudoin-Massiani, O., Stuttem, I. & Schweisguth, F. (2004) *Development (Cambridge, U.K.)* **131,** 469–478.
36. Bastock, R., Strutt, H. & Strutt, D. (2003) *Development (Cambridge, U.K.)* **130,** 3007–3014.
37. Wong, L. L. & Adler, P. N. (1993) *J. Cell Biol.* **123,** 209–221.
38. Fremion, F., Astier, M., Zaffran, S., Guillen, A., Homburger, V. & Semeriva, M. (1999) *J. Cell Biol.* **145,** 1063–1076.
39. Jones, K. H., Liu, J. & Adler, P. N. (1996) *Genetics* **142,** 205–215.
40. Chen, C. M. & Struhl, G. (1999) *Development (Cambridge, U.K.)* **126,** 5441–5452.
41. Strapps, W. R. & Tomlinson, A. (2001) *Development (Cambridge, U.K.)* **128,** 4829–4835.
42. Chen, C. M., Strapps, W., Tomlinson, A. & Struhl, G. (2004) *Proc. Natl. Acad. Sci. USA* **101,** 15961–15966.
43. Klaes, A., Menne, T., Stollewerk, A., Scholz, H. & Klambt, C. (1994) *Cell* **78,** 149–160.
44. Brand, A. H. & Perrimon, N. (1993) *Development (Cambridge, U.K.)* **118,** 401–415.
45. Nolo, R., Abbott, L. A. & Bellen, H. J. (2000) *Cell* **102,** 349–362.
46. Gho, M., Lecourtois, M., Geraud, G., Posakony, J. W. & Schweisguth, F. (1996) *Development (Cambridge, U.K.)* **122,** 1673–1682.
47. Wieshaus, E. & Nusslein-Volhard, C. (1996) in *Drosophila: A Practical Approach*, ed. Roberts, D. B. (IRL, Oxford), pp. 199–227.
48. Carty, D. J. & Iyengar, R. (1994) *Methods Enzymol.* **237,** 38–44.